Semiconductor Electrodes

XLI. Improvement of Performance of n-WSe_2 Electrodes by Electrochemical Polymerization of o-Phenylenediamine at Surface Imperfections

Henry S. White, Hector D. Abruna, and Allen J. Bard*

Department of Chemistry, The University of Texas at Austin, Austin, Texas 78712

ABSTRACT

The dark electrochemical polymerization of o-phenylenediamine (OPD) at n-WSe_2 and n-$MoSe_2$ single crystal electrodes (surface $\perp$C axis exposed) was investigated. The results indicate that polymerization occurs only at surface imperfections (edges, steps) in the otherwise smooth van der Waal's surface. The photoelectrochemical response, in aqueous solutions containing $Fe(CN)_6^{3-}$/$Fe(CN)_6^{4-}$ and I_3^-/I^-, of electrodes subjected to this polymerization is improved compared to the untreated electrodes. The results are consistent with a decrease in recombination rate due to blocking of surface states by OPD polymerization. The characteristics of several PEC cells before and after OPD polymerization are also described. Increases in the solar-to-electrical power efficiency, η, range from 30-300% after surface pretreatment.

The nature of the surface of a semiconductor electrode in a photoelectrochemical cell (PEC) plays an important role in the efficiency of conversion of impinging radiant energy into net external current (1). Much of the success in recent years in improvement of PEC performance can be attributed to the discovery of etching procedures or chemical treatments which decrease the extent of recombination reactions at the semiconductor electrode. The layered semiconductor materials, *e.g.*, $MoSe_2$ and WSe_2, while promising candidates as electrodes for PEC's, frequently show large energy losses via recombination processes at crystal imperfections in the photoactive surface ($\perp$C axis) (1a, 2-7). These recombination centers show metallic-like behavior in that dark oxidation and reduction of solution species with redox potentials corresponding to energies between the valence band and conduction edges is quite facile at electrodes with exposed edges on the surface. Parkinson and co-workers (6, 7) have taken advantage of the intercalation properties of these layered materials to attach bulky molecular species at the edges to block these recombination centers and thus prevent electron exchange with solution species. This method improved the overall energy conversion characteristics of PEC's based on n-WSe_2 and $MoSe_2$ in aqueous I^-/I_3^- solutions.

We report here an alternative approach to blocking the recombination associated with surface imperfections of n-WSe_2 and n-$MoSe_2$ electrodes by the dark electrochemically initiated polymerization of an impervious coating at these sites. The strategy here is based on the fact that only the recombination sites on n-type materials allow appreciable dark anodic currents. The oxidation of ortho-phenylenediamine (OPD) at metallic electrodes yields a polymeric product that effectively blocks the electrode surface (8-10), and prevents electron exchange with solution species. The use of this polymerization reaction at the surface imperfections of layered crystals provides for the specific passivation of recombination centers.

A simplified representation of the strategy involved here is shown in Fig. 1. In the absence of surface states or deep traps electrons generated within the space-charge region are driven to the bulk of the electrode where they are collected at the rear ohmic contact or recombine with minority carriers. When surface states are present (Fig. 1a) that can trap photogenerated carriers, either direct recombination of electron-hole pairs may occur or the electrons may reduce photogenerated products (*e.g.*, I_3^-) if they are energetic enough (*i.e.*, highly reducing) and have an accessible pathway to the solution (11). This latter recombination process plays a significant role in limiting solar conversion efficiencies of photoelectrochemical systems based on WSe_2 and $MoSe_2$ since the empty metallic d-orbitals that comprise the conduction band can shunt photogenerated electrons to solution species at surface imperfections. The effect of OPD dark oxidation is to increase the resistance of the electron pathway between the conduction band and solution and thereby decrease the recombination rate. The result of blocking these surface imperfections of n-WSe_2 and n-$MoSe_2$ crystals on the photooxidation of I^- and $Fe(CN)_6^{4-}$ is demonstrated.

Experimental

Single crystals of n-WSe_2 were donated by Dr. Barry Miller and Dr. Frank DiSalvo (Bell Labs). The n-$MoSe_2$ sample was a gift from Mr. Ying-sheng Huang (Boston College). Ohmic contacts were made by rubbing In/Ga onto the back of the crystals which were then attached with conductive silver paint to a copper lead and mounted on 6 mm bore glass tubing. The elec-

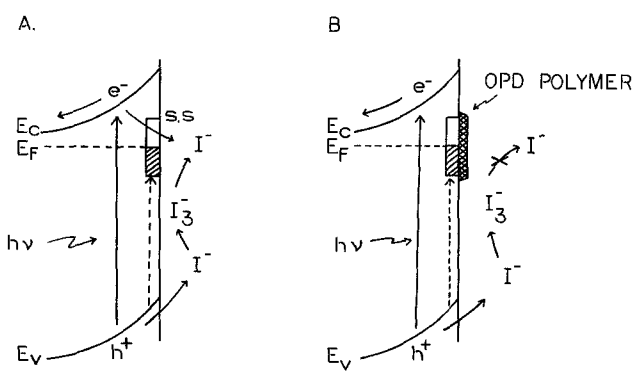

Fig. 1. Schematic representation of the effect of OPD dark oxidation on the semiconductor/solution interface. A. Before OPD oxidation showing reduction of photooxidized product (I_3^-) by electrons shunted to solution through surface state (s.s.). B. After OPD polymerization: showing blockage of solution species to surface state. E_c = conduction bandedge, E_F = Fermi level, E_V = valence bandedge. Dashed line in A and B indicates direct electron-hole recombination by surface state.

* Electrochemical Society Active Member.

Key words: photoelectrochemical, efficiencies, electrochemical polymerization.

trodes were masked with 5 min epoxy cement and sealed in wax except for the surface to be illuminated. The area of the exposed surfaces ranged from 0.20-0.02 cm^2. As discussed below, the degree of surface imperfection varied considerably from sample to sample. No attempt was made to measure quantitatively the percentage of exposed surface area composed of edges, steps, or other imperfections. Some crystals had a considerable number of clusters composed of microcrystals, ~10 μm^2, attached to the exposed surface, as found by scanning electron microscopy (SEM).

O-phenylenediamine (1,2-diaminobenzene) was recrystallized three times from methylene chloride and stored under N_2 in the dark. Triply distilled water was used throughout. All other chemicals were used without further purification.

The electrochemical cells and apparatus have been previously described (4). All potentials are reported *vs.* a sodium saturated calomel electrode (SSCE). A Spectraphysics He/Ne laser (80 mW/cm^2, at 632.8 nm), an Oriel Corporation (Stamford, Connecticut) 450W xenon lamp (power of focused beam ~150 mW/cm^2), or a commercial sunlamp (~60 mW/cm^2) were used to irradiate the photoelectrodes. The power of the light sources was measured with an E. G. & G. (Salem, Massachusetts) Model 550 radiometer/photometer and a Scientech 361 power meter. The light intensity at the electrode surface was varied with neutral density filters (Oriel Corporation).

Results

Platinum.—The electrochemical oxidation of the isomeric phenylenediamines has been the subject of a number of investigations (8-10). Oxidation of OPD leads to the production of a nonconductive film on the electrode surface. This effect can be seen in the cyclic voltammetric response of a Pt disk electrode in contact with a 25 mM o-phenylenediamine, 0.2M Na_2SO_4 solution (borate buffer, pH 9.1) (Fig. 2a). As indicated by the decreasing currents upon consecutive potential scans, OPD oxidation leads to a coating which effectively blocks the metal surface. The thickness of the polymeric coating measured on Pt after 20 consecutive potential scans was 1-2 μm, as measured with a Dektak Profilometer. To assess the extent of blockage, the cyclic voltammetric response of the coated electrodes was examined in solutions containing a high concentration of electroactive species [0.4M $Fe(CN)_6^{4-}$/0.05M $Fe(CN)_6^{3-}$ and 1.0M I^-/0.05M I_2] which are typical of solutions employed in liquid junction solar cells. The results are presented in Table I. Although OPD polymer films on Pt nearly completely block oxidation of $Fe(CN)_6^{4-}$ and reduction of $Fe(CN)_6^{3-}$, a much smaller blocking effect was found in I^-/I_3^- solutions. The smaller decrease in current caused by the polymeric film for I_3^- reduction and I^- oxidation can probably be attributed to some partitioning of these species into the film.

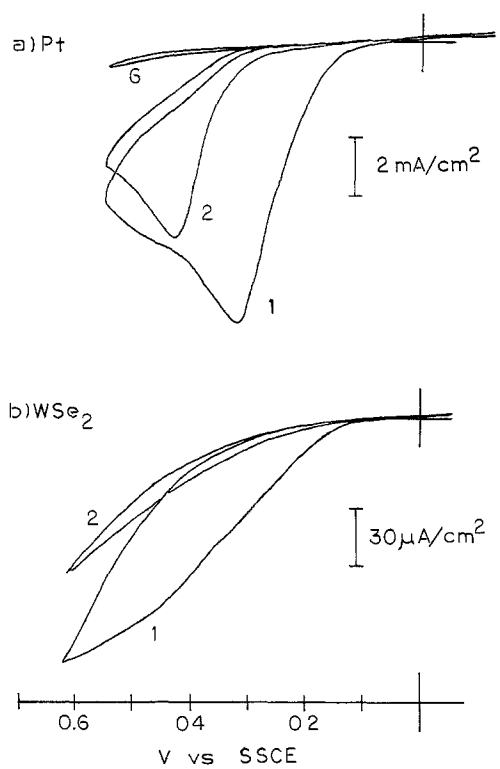

Fig. 2. (a) Voltammetric response of a Pt disk electrode in 25 mM o-phenylenediamine (0.2M Na_2SO_4, borate buffer, pH 9.1), scan rate = 100 mV/sec. (b) Dark voltammetric response of n-WSe_2 under the same conditions. Numbers on curves refer to the scan number.

To obtain a better idea of the nature of the blockage of the electrochemistry of solution reactants, potential step experiments were conducted on platinum electrodes bearing polymeric films of OPD in solutions of $Fe(CN)_6^{3-/4-}$ and I^-/I_3^-. In all cases, the potential was stepped sufficiently beyond the diffusion plateau (typically 200-300 mV) to insure diffusion-limited behavior. With $Fe(CN)_6^{3-/4-}$ (0.05 and 0.38M, respectively), good Cottrell behavior (*i.e.*, a linear plot of i *vs.* $t^{-1/2}$) was found for $t < 20$ sec. However, for $20 > t > 30$ sec, a sudden drop in current was observed after which a very slow decrease in current ensued. This behavior was reproducible for a number of specimens and for different step sizes (provided the final potential was past the diffusion plateau). This behavior can be accounted for by assuming that at short times, there is sufficient electroactive material inside the polymer film to insure Cottrell behavior. At longer times, this material is depleted (current drop) and thereafter the response is controlled by slow diffusion through the polymer film (membrane-controlled diffusion). A model for this behavior has been proposed (12). Given this, it is instructive to contrast the transient *vs.* the steady-state behavior and their relation to PEC cells. Thus, although on a cyclic voltammetric time scale (say at 100 mV/sec) the decrease in current associated with the polymer film may not appear to be very large, the steady-state current that can be sustained will be much smaller at the polymer-coated electrode than at the bare electrode. Since in operating PEC's it is the steady state and not the transient current flow that is relevant in these systems, cyclic voltammetry experiments will, in general, not be a true reflection of the degree of passivation of recombination sites. Thus, Fig. 3, 4, and 5 represent a lower limit of the degree of passivation of recombination centers.

For I^-/I_3^- (1.0 and 0.05M, respectively) the results are somewhat different. Even on a bare, freshly polished Pt electrode, the oxidation of I^- shows some peculiarities, *i.e.*, after a potential step (*e.g.*, 0 to 0.6V)

Table I. Steady-state currents at bare Pt and Pt/OPD electrodes

Solution	$E_{1/2}$ (V *vs.* SSCE)	i (Pt)* (μA)	i (Pt/OPD)** (μA)	% Decrease
0.39M $Fe(CN)_6^{4-/3-}$,		[Oxidation (+0.5V)]		
0.05M $Fe(CN)_6^{-3}$	0.23V	560	1	>99
		[Reduction (0.0V)]		
		65	1.5	98
1.9M I^-, 0.05M I_2		[Oxidation (+0.6V)]		
	0.27V	940	150	84
		[Reduction (0.0V)]		
		32	24	25

* Polished Pt electrode.
** Electrode coated with polymer formed on oxidation of OPD.

the current rises rapidly and then starts to decay. It then undergoes periodic oscillations in the current centered around a relatively stable steady-state value. This phenomenon has been ascribed to the formation and subsequent removal of solid iodine films on the surface of the electrode. A qualitatively similar behavior is observed for polymer-coated electrodes except that the currents are decreased by a factor of *ca.* 10. For I_3^- reduction, both the bare and the polymer-coated electrodes show smoothly decaying current-time profiles with the latter showing currents which are suppressed by *ca.* 20%. The results can be interpreted as being mainly due to the differences in permeability of I^- and I_3^- in the polymer film. Since I^- has a much higher charge density than I_3^-, it will show a lower permeability through the polymeric film, and the oxidation current at the polymer modified electrode will be greatly suppressed (as found with the $Fe(CN)_6^{3-/4-}$ system). However, I_3^- is able to penetrate the film much more easily and as a result, only a moderate decrease in current is observed when compared to the bare electrode. These interpretations are consistent with observations made on the permeability of redox reagents through polymeric films (12).

It should be noted that the OPD polymeric film (pK_a 4.5) is capable of acting as an ion exchange film in the protonated form at lower *p*H and, in fact, the acid/base properties of OPD films on Pt electrodes have been suggested for use as potentiometric sensors (10). Only a small difference was observed in the blocking ability of the film in $Fe(CN)_6^{3-/4-}$ solutions over the *p*H range of 2-14.

The electrochemical polymerization of OPD at platinum is also strongly dependent on *p*H. The passivation of the electrode surface occurs at a rate that increases with decreasing *p*H. At *p*H 2 (trifluoroacetate buffer) only 2-3 potential scans were necessary to reduce the current to <5% of the initial peak value while at *p*H 9.1, approximately 10 scans were necessary. The films obtained at *p*H 6-10 had the largest blocking effect in $Fe(CN)_6^{4-/3-}$ and I^-/I_3^- solutions. Except where noted, the results reported here were obtained at *p*H 9.1 (sodium borate buffer) with 0.2M Na_2SO_4. The OPD coated Pt electrodes (Pt/OPD) appear to be quite stable. No increase in current was observed after 15-20 hr of continuous operation in $Fe(CN)_6^{3-/4-}$ or I^-/I_3^- solutions. This was done in a steady-state fashion by holding the electrode potential 200 mV positive of the standard potential for the redox couple in question.

Semiconductor electrodes.—A typical cyclic voltammogram for OPD (25 mM) oxidation in the dark at an n-WSe_2 electrode is shown in Fig. 2b. All OPD oxidations at the semiconductor electrodes were performed in the dark to prevent polymer formation on the photoactive surface. Comparison of Fig. 2a and 2b demonstrates that blocking of the dark electrochemical (recombination) sites is quite similar to that at a metallic surface. As expected, the current densities calculated on the basis of the geometric areas were smaller at the semiconductor electrodes since the area included the surface $\perp$C axis which is nonactive in the dark. However, the voltammetric response is qualitatively very similar to Pt. Blockage of the surface imperfections, as indicated by the decreasing currents, occurred at a slower rate than at Pt. After cycling between 0.0 and +0.6V (10-20 scans at 20 mV/sec), the dark current was reduced to 5-50% of the initial value. The difference in the initial and final currents strongly depended on the initial quality of the electrode surface; electrodes with many imperfections showed the biggest decrease. SEM photographs of Pt surfaces after OPD polymerization revealed a fairly smooth surface with scattered islands of a microcrystalline product. Similarly, SEM photographs of n-WSe_2 electrodes after OPD dark polymerization were featureless except for very similar crystalline product aggregates found at imperfections on the van der Waal's plane. These crystals were easily distinguished from the larger microcrystals of n-WSe_2 sometimes found on the electrode surface. The crystalline OPD oxidation product was absent from the smoother portions of electrode surface indicating that dark oxidation of OPD does not occur at the photoactive surface.

Effect of OPD polymerization on photoelectrochemical response.—The desired voltammetric characteristics of a photoanode in contact with a concentrated solution of oxidizable material are as follows: (*i*) the potential for onset of photocurrent, V_{onset}, should be as negative as possible and limited by the flatband potential; (*ii*) photocurrents should be limited by the light intensity and be potential independent at potentials positive of V_{onset}. Figures 3 and 4 are illustrations of the voltammetric behavior in the dark and under illumination of two n-WSe_2 electrodes in unstirred 1.0M I^-/0.05M I_3^- solutions before and after dark oxidation of OPD. The surface quality of these electrodes varied considerably with the one in Fig. 4, having a much smaller concentration of surface defects. A similar experiment performed in a solution containing 0.7M $Fe(CN)_6^{4-}$, 0.05M $Fe(CN)_6^{3-}$ is shown in Fig. 5. In all three cases, a significant improvement in the voltammetric photoresponse was observed after dark oxidation of OPD. The dark reduction current (which would represent a recombination of photogenerated oxidized species) decreased and the photocurrent increased. The degree of improvement varied considerably from sample to sample. However, the largest increases in photocurrent (i_{photo}) and most negative shifts of V_{onset} were observed at electrodes with the poorest initial response (compare Fig. 3 and 4). In addition, the photocurrent became much less potential dependent beyond V_{onset} and the *i*-*V* curves showed better fill factors. Furthermore, less hysteresis was observed in the photocurrent

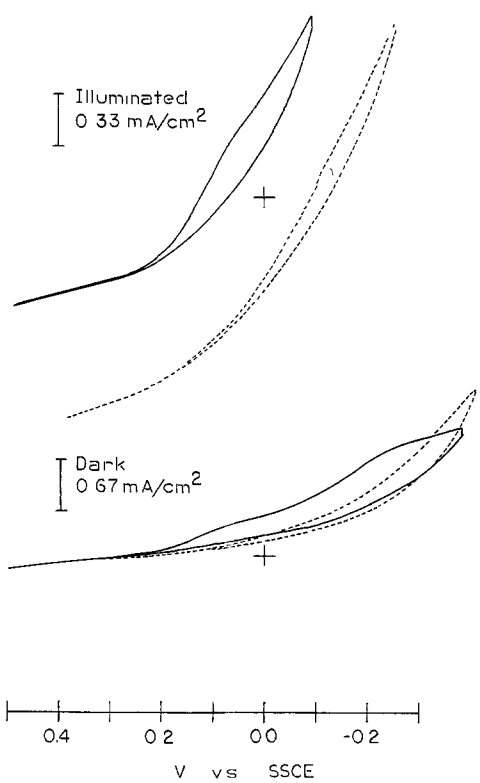

Fig. 3. Voltammetric response of n-WSe_2 in the dark and under illumination in 1.0M NaI, 0.05M I_2 (borate buffer, *p*H 9.1) before (solid lines) and after (dashed lines) dark OPD oxidation. Input power was 60 mW/cm² (commercial sunlamp), scan rate = 100 mV/sec.

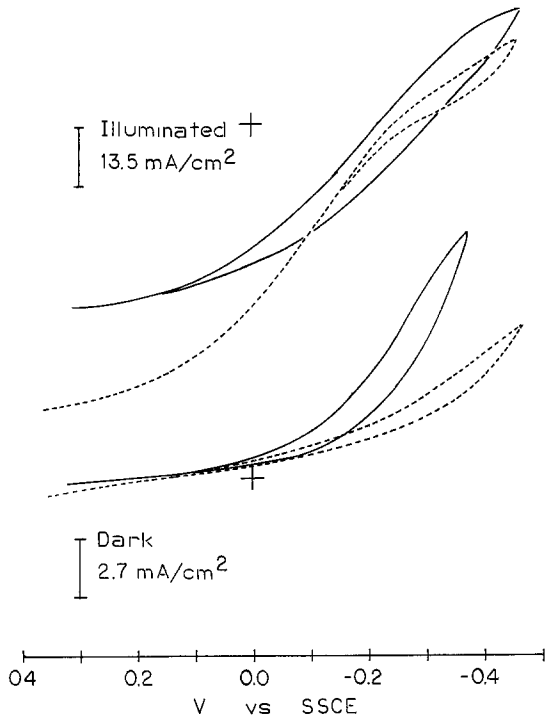

Fig. 4. Voltammetric response of n-WSe_2 in the dark and under illumination in 1.0M NaI, 0.05M I_2 (borate buffer, pH 9.1) before (solid lines) and after (dashed lines) OPD dark oxidation. Input power of 450W xenon lamp was 150 mW/cm², scan rate = 100 mV/sec.

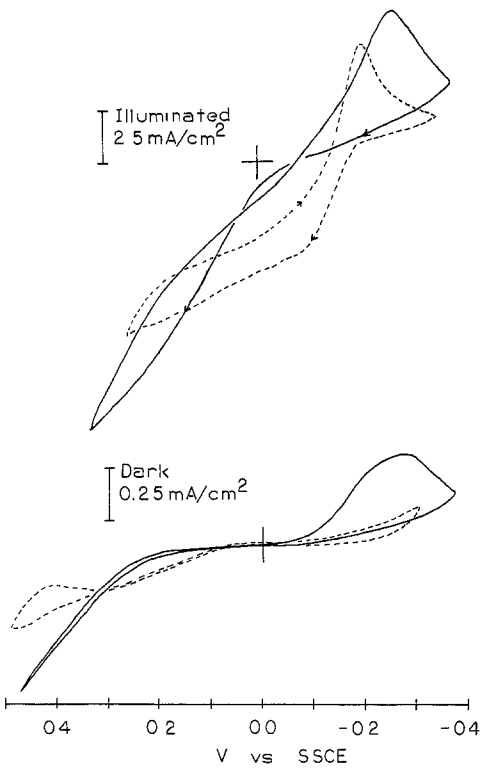

Fig. 5. Voltammetric response of n-WSe_2 in the dark and under illumination in 0.7M $K_4Fe(CN)_6$, 0.05M $K_3Fe(CN)_6$ (borate buffer, pH 9.1) before (solid lines) and after (dashed lines) dark OPD oxidation. Input power of He/Ne laser was 80 mW/cm², scan rate = 100 mV/sec.

voltammograms, especially in the potential region ~0.3V positive of V_{onset}.

The voltammetric behavior of the semiconductor electrodes in I^-/I_3^- and $Fe(CN)_6^{4-/3-}$ solutions after OPD polymerization was characterized by dark cathodic currents at potentials negative of V_{onset} that were considerably smaller after the pretreatment (see Fig. 3-5). There was a small increase of the dark anodic current in the 0.1-0.3V region following the OPD treatment. This may be caused by a small amount of continued oxidation of OPD monomer or electroactive species entrapped in the film.

Current-potential scans under chopped illumination (for light pulses of 1-2 sec) were especially useful in diagnosing the effect of OPD treatment. Such an *i*-V trace for the electrode used in Fig. 4 is shown in Fig. 6. Sudden illumination of an untreated electrode in the potential region 0.0 to −0.3V *vs.* SSCE resulted in a photoanodic current that decayed rapidly with time. A corresponding cathodic transient was observed in this potential region immediately after blocking the light source. When the light was chopped at a fixed potential, the *i*-*t* transient showed a more pronounced current decay (see inset, Fig. 6). After dark OPD polymerization, the photocurrents were not only larger, but the transient current decay observed after illuminating and blocking the light was noticeably reduced. The magnitude of the cathodic dark current recorded after blocking the light source was also reduced. It is clear that the transient nature of the photocurrent observed before OPD oxidation is not due to depletion of I^- at the electrode surface since the decay is not observed at the higher initial currents after OPD oxidation.

To contrast the effect of blocking only the recombination sites by dark oxidation of OPD, we also investigated the OPD oxidation on an illuminated n-WSe_2 electrode. The oxidation of OPD at n-WSe_2 under constant illumination (80 mW/cm²) begins at −0.25V *vs.* SSCE. A peak current of 0.7 mA/cm² was observed at 0.2V during the initial forward scan (100

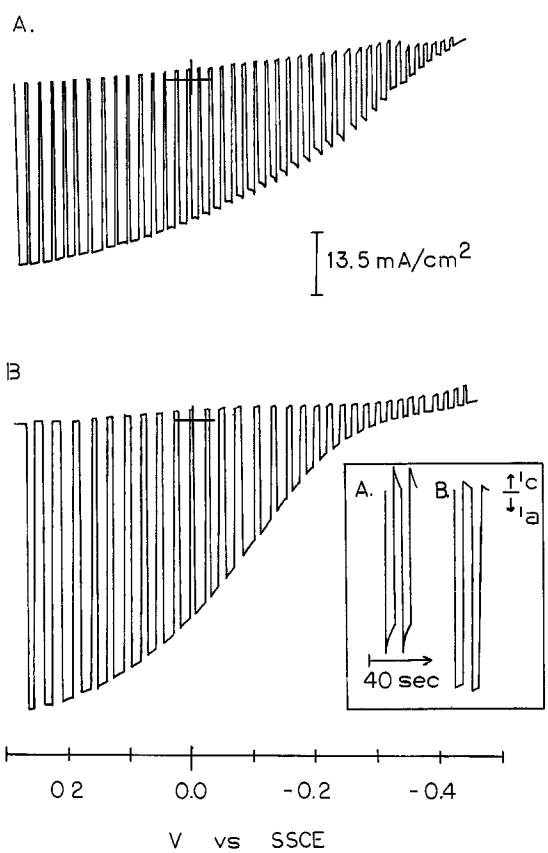

Fig. 6. Voltammetric response under chopped illumination for the electrode represented in Fig. 4. n-WSe_2 in 1.9M NaI, 0.5M I_2 (borate buffer, pH 9.1) before (A) and after (B) OPD dark oxidation. Inset shows i-t response under chopped illumination at fixed potential (−0.1V). Input power of 450W xenon lamp was 150 mW/cm², scan rate = 10 mV/sec.

mV/sec), but decreased by ~90% on the second scan indicating blockage of the photoactive surface. The integrated current for the oxidation of OPD corresponded to a surface coverage of *ca.* 3×10^{-8} mol/cm² (based on a $1e^-$ oxidation and assuming that none of the oxidation product dissolved). The voltammetric response of this electrode in 0.7M $Fe(CN)_6^{4-}$ solution showed a 95% decrease in photocurrent as compared to a measurement made before a photopolymerization.

Photoelectrochemical cells (PEC's).—The results of several photoelectrochemical cells tested before and after OPD oxidation are listed in Tables II and III. The *i-V* curves, along with i_{sc} (short-circuit photocurrent) and V_{oc} (open-circuit photovoltage) as a function of light intensity for three PEC's are shown in Fig. 7-9. As expected from the voltammetric behavior, increases in i_{sc} and/or V_{oc} were observed for these cells after OPD oxidation with largest improvements occurring for electrodes that initially performed rather poorly. A 30-50% increase in η, the power conversion efficiency, represents the general range of improvement due to pretreatment, although an increase in η as high as 317% was observed for the $Fe(CN)_6^{4-/3-}$ cell shown in Fig. 7.

Plots of short-circuit photocurrent, i_{sc}, and open-circuit photovoltage, V_{oc}, as a function of light intensity provide additional insight into the effect of OPD oxidation. In the n-WSe_2/$Fe(CN)_6^{4-/3-}$/Pt cell represented in Fig. 7, i_{sc} saturates at the relatively low light intensity of 30 mM/cm², before OPD polymerization. After treatment the photocurrent increases linearly with light intensity to 55 mW/cm² before saturation ensues. V_{oc} for the same electrode increased by 0.1V after polymerization, although the saturation value was reached at relatively low light intensity (15 mW/cm²) regardless of the surface treatment. The fill factor for this cell increased from 0.15 to 0.36 after treatment.

The OPD pretreatment is also beneficial with other layered semiconductors, such as n-$MoSe_2$. The characteristics of an n-$MoSe_2$/I^-, I_3^-/Pt PEC represented in Fig. 8 show a different effect of OPD dark oxidation. Initially, the current showed a linear increase with light intensity up to the full lamp output (80 mW/cm²) and i_{sc} increased slightly after polymerization. However, before polymerization, V_{oc} did not reach a limiting value even at full illumination intensity, whereas after OPD oxidation, it saturated at quite low light intensity, 20 mW/cm², although at a slightly lower value. The fill factor for this cell, however, increased from 0.40 to 0.52.

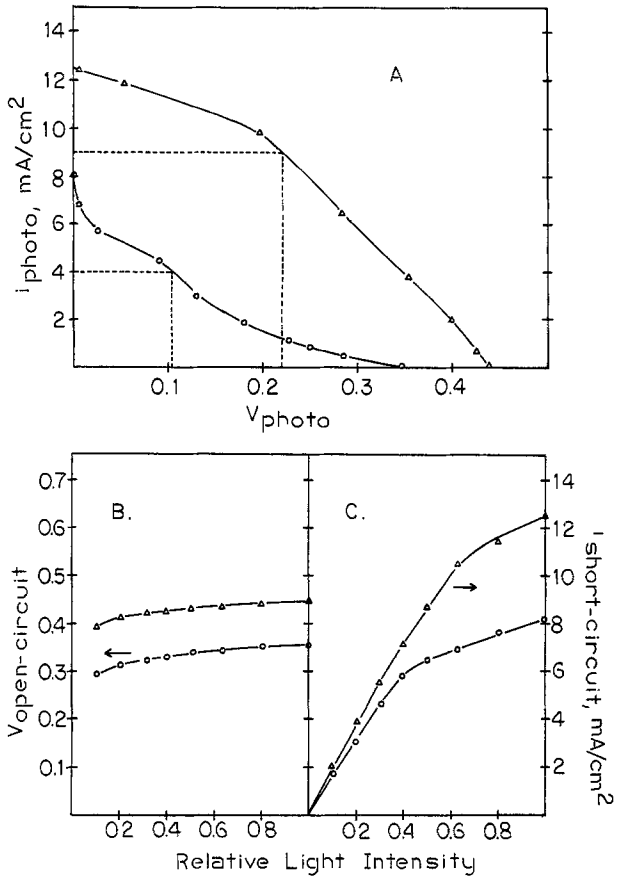

Fig. 7. Photocharacteristics of n-WSe_2/0.7M $K_4Fe(CN)_6$, 0.05M $K_3Fe(CN)_6$ (borate buffer, pH 9.1)/Pt PEC. (A) *i-V* curve before (○) and after (△) dark OPD oxidation. Intersection of dashed lines indicates the maximum power point. (B) Open-circuit photovoltage and (C) short-circuit photocurrent as a function of light intensity before (○) and after (△) OPD dark oxidation. Input power of He/Ne laser at 637.8 nm = 80 mW/cm².

Finally, the characteristics of an n-WSe_2/I^-, I_3^-/Pt PEC are depicted in Fig. 9. In this case, while V_{oc} was

Table II. Effect of OPD polymerization on i_{sc} and V_{oc}

Electrode	Solution	i_{sc} (before) (mA/cm²)	i_{sc} (after) (mA/cm²)	% Increase	V_{oc} (before) (V)	V_{oc} (after) (V)	% Increase
WSe_2 No. 1*	0.7M $Fe(CN)_6^{4-}$	8.0	12.5	56	0.35	0.44	26
WSe_2 No. 2*	0.7M $Fe(CN)_6^{4-}$	6.3	6.3	0	0.39	0.49	26
WSe_2 No. 3*	0.7M $Fe(CN)_6^{4-}$	3.8	12.0	216	0.45	0.47	4
WSe_2 No. 4**	1M I^-/0.05M I_3^-	43	44	2	0.64	0.64	0
WSe_2 No. 5†	1M I^-/0.05M I_3^-	0.55	1.3	136	0.21	0.39	86
WSe_2 No. 6*	1M I^-/0.05M I_3^-	5.6	7.5	33	0.29	0.40	38
WSe_2 No. 7**	1M I^-/0.05M I_3^-	22.8	28.3	24	0.52	0.55	6
WSe_2 No. 8**	1M I^-/0.05M I_3^-	40.5	61.6	52	0.54	0.56	4
$MoSe_2$ No. 1*	1M I^-/0.05M I_3^-	10.5	14	18	0.48	0.45	−6

* Irradiation with 1.6 mW He/Ne laser (~80 mM/cm²).
** Irradiation with 450W xenon lamp (focused power ~150 mW/cm²).
† Irradiation with sunlamp (~60 mW/cm²).

Table III. Effect of OPD polymerization on fill factor (f.f.), quantum efficiency (Φ), and power efficiency (η)

Electrode	Solution	f.f. (before)	f.f. (after)	Φ (%) (before)	Φ (%) (after)	η (%) (before)	η (%) (after)	Relative η change (%)
WSe_2 No. 1	$Fe(CN)_6^{4-/3-}$	0.18	0.36	20	30	0.6	2.5	317
WSe_2 No. 8*	I^-/I_3^-	0.34	0.32	45	69	5.0	7.4	28
WSe_2 No. 7*	I^-/I_3^-	0.33	0.33	25	32	2.6	3.4	31
WSe_2 No. 6**	I^-/I_3^-	0.33	0.37	14	19	0.7	1.4	100
$MoSe_2$ No. 1**	I^-/I_3^-	0.40	0.52	24	34	2.5	3.9	56

* He/Ne laser.
** 450W xenon lamp.

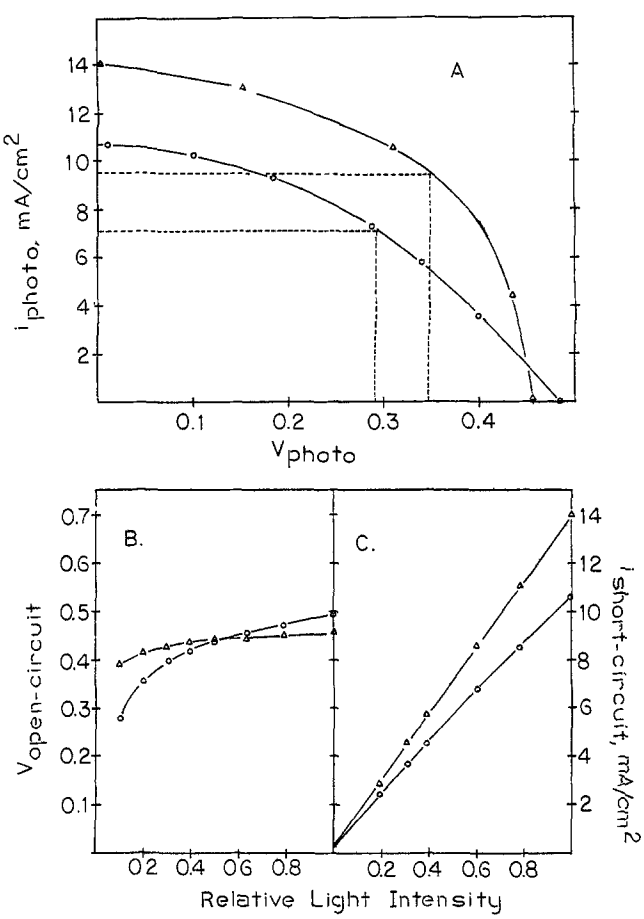

Fig. 8. Photocharacteristics of n-$MoSe_2$/1.0M NaI, 0.05M I_2 (borate buffer, pH 9.1)/Pt PEC. (A) i-V curve before (○) and after (△) dark OPD oxidation. Intersection of dashed lines indicates the maximum power point. (B) Open-circuit photovoltage and (C) short-circuit photocurrent as a function of light intensity before (○) and after (△) OPD dark oxidation. Input power of He/Ne laser at 632.8 nM = 80 mW/cm^2.

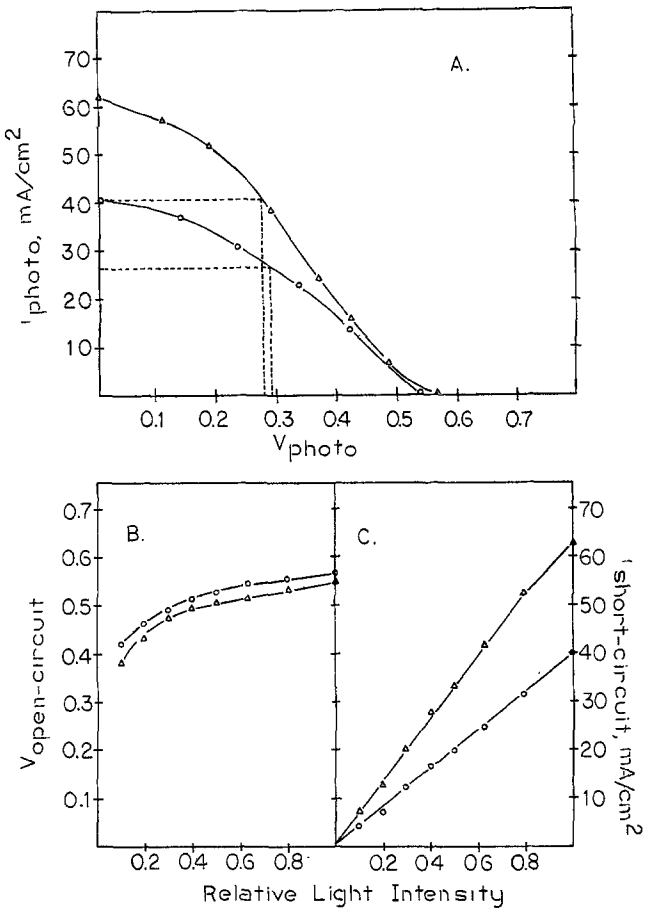

Fig. 9. Photocharacteristics of n-WSe_2/1.0M NaI, 0.05M I_2 (borate buffer, pH 9.1)/Pt PEC. (A) *i-V* curve before (○) and after (△) dark OPD oxidation. Intersection of dashed lines indicates the maximum power point. (B) Open-circuit photovoltage and (C) short-circuit photocurrent as a function of light intensity before (○) and after (△) OPD dark oxidation. Total input power of 450W xenon lamp = 150 mW/cm^2.

not significantly affected by OPD oxidation, a large increase in i_{sc} was observed. The *i-V* photocurve revealed a large increase in i_{photo} at photovoltages less than 0.4V after OPD oxidation. This same effect can be observed in the voltammetric response, Fig. 4 and 6.

The stability of the semiconductor/OPD electrodes was tested in PEC cells operated at short circuit in I^-/I_3^- solutions. No decrease in i_{sc} or V_{oc} was observed after 20 hr of continuous operation at near the maximum power point.

Discussion

The surface recombination and energy losses occurring at imperfections in the van der Waal's plane of layered semiconducting materials has been discussed in several recent papers (1-7). Transition metal atoms, exposed to the solution by surface defects, allow the back reaction of the photogenerated products to occur (dark reductions at n-type materials) resulting in decreases in the solar conversion efficiency (3, 5-7). These defects may also act as direct recombination centers of photogenerated charge carriers (electron-hole pairs) (2) although this process is less discernible from the voltammetric response.

The flatband potential, V_{FB}, of n-WSe_2 samples measured in aqueous solutions is −0.3 to −0.4V *vs.* SCE (4). As shown in Fig. 3-5, a relatively large dark current due to reduction of I_3^- or $Fe(CN)_6^{3-}$ is observed on untreated samples at potentials positive of this value. The magnitude of these currents at a continuously illuminated surface is not measurable from the experiments performed here since only a net photoanodic current is observed. However, because the surface concentration of the photogenerated oxidized product is higher than the bulk concentration and this product can be reduced at surface imperfections, considerably higher cathodic currents would be expected under illumination than those measured in the dark. The effect of OPD polymerization clearly is to block this back reaction and thus produce a larger net anodic photocurrent. In this manner, the polymeric product due to OPD oxidation acts as a selective sealant, blocking the approach of solution species to the dark electroactive sites (surface states) within the bandgap, Fig. 1.

While Fig. 1a depicts a simplified view of the overall reactions involved in recombination processes, the rate of back reaction will be clearly dependent on the density and energy distribution of surface levels as well as on the kinetics for charge transfer. Since a qualitative correlation exists (2, 3, 5) between the degree of surface imperfection and the dark and photoresponse of these electrode materials, it can be safely ascertained that the lower-than-ideal efficiencies for solar energy conversion is due, at least in part, to recombination reactions associated with those surface states. Limited band-bending within the space-charge region due to Fermi level pinning (5, 13) or inversion (14) is an additional source of energy loss in these materials. We address the former problem by the use of materials that can selectively block these recombination sites and thereby minimize losses associated with them.

Since the improvement in performance is based on the blockage of surface states upon dark oxidation at an n-type material, there are some restrictions on the potential required to initiate the polymerization. If

the energy level for polymerization (E_{pol}) is above E_c, then dark oxidation on the photoactive surface may be possible with subsequent blockage of useful surface. If E_{pol} is too far below the energy level of the surface states, E_{ss} (*i.e.* the polymerization occurs at too positive potentials), dark oxidation via surface states may not be possible. Thus, the optimum energies (eV) for the oxidation reaction producing polymer lies at $E_{ss} > E_{pol} > E_c$. The polymerization of OPD at n-WSe_2 lies within this energy range (*i.e.*, within the upper third of the bandgap). Clearly other materials that undergo electrochemical polymerization may also be suitable candidates for study.

This approach may prove to be a way for improving the efficiency of not only single crystal layered materials but also of polycrystalline ones. Work along these lines is the subject of current efforts in our laboratories.

Acknowledgment

The assistance of Dr. Michael Schmerling in obtaining electron micrographs is gratefully acknowledged. This work was supported by the National Science Foundation (CHE 8000682) and the Solar Energy Research Institute.

Manuscript submitted July 30, 1981; revised manuscript received Sept. 28, 1981.

Any discussion of this paper will appear in a Discussion Section to be published in the December 1982 JOURNAL. All discussions for the December 1982 Discussion Section should be submitted by Aug. 1, 1982.

Publication costs of this article were assisted by The University of Texas at Austin.

REFERENCES

1. See (a) A. J. Bard, F.-R. F. Fan, A. S. Gioda, G. Nagasubramanian, and H. S. White, *Discuss. Faraday Soc.*, **70**, 19 (1980); (b) B. A. Parkinson, A. Heller, and B. Miller, *J. Appl. Phys.*, **33**, 5231 (1978); (c) B. A. Parkinson, A. Heller, and B. Miller, *This Journal*, **126**, 954 (1979) and references therein.
2. H. J. Lewerenz, A. Heller, and F. J. DiSalvo, *J. Am. Chem. Soc.*, **102**, 1877 (1980).
3. (a) W. Kautek, H. Gerischer, and H. Tributsch, *Ber. Bunsenges. Phys. Chem.*, **83**, 1000 (1979); (b) S. M. Ahmed and H. Gerischer, *Electrochim. Acta*, **24**, 703 (1979).
4. F.-R. F. Fan, H. S. White, B. L. Wheeler, and A. J. Bard, *J. Am. Chem. Soc.*, **102**, 5142 (1980).
5. H. S. White, F.-R. F. Fan, and A. J. Bard, *This Journal*, **128**, 1045 (1981).
6. D. Canfield and B. A. Parkinson, *J. Am. Chem. Soc.*, **103**, 1281 (1981).
7. B. A. Parkinson, T. E. Furtak, D. Canfield, K. Kam, and G. Kline, *Discuss. Faraday Soc.*, **70**, (1980).
8. (a) R. N. Adams, "Electrochemistry at Solid Electrodes," p. 360, Marcel Dekker, Inc., New York (1969); (b) H. Y. Lee and R. N. Adams, *Anal. Chem.*, **34**, 1587 (1962).
9. A. M. Yacynych and H. B. Mark, *This Journal*, **123**, 1346 (1976).
10. W. R. Heineman, H. J. Wieck, and A. M. Yacynych, *Anal. Chem.*, **52**, 345 (1980).
11. (a) P. A. Kohl and A. J. Bard, *J. Am. Chem. Soc.*, **99**, 7531 (1977); (b) F.-R. F. Fan and A. J. Bard, *ibid.*, **102**, 3677 (1980).
12. P. Peerce and A. J. Bard, *J. Electroanal. Chem. Interfacial Electrochem.*, **112**, 97 (1980).
13. L. F. Schneemeyer and M. S. Wrighton, *J. Am. Chem. Soc.*, **102**, 6964 (1980).
14. W. Kautek and H. Gerischer, *Ber. Bunsenges. Phys. Chem.*, **84**, 645 (1980).

The Nature of Passivation of Lead Sulfide during Anodic Dissolution in Hydrochloric Acid

Balasubramaniam Dandapani* and Edward Ghali*

Department of Mining and Metallurgy, Laval University, Quebec, Canada G1K 7P4

ABSTRACT

Effective electrowinning of lead directly from its sulfide ore requires a fundamental understanding of its electrodissolution process. Studies made on the anodic dissolution of PbS in hydrochloric acid have shown that there are obstructions to the electrodissolution due to some passivation. Detailed surface examination (SEM-EDAX and x-ray diffraction studies) is conducted to determine the nature of the passivation products at various potential regions. It has been shown that crystalline sulfur, lead chloride, and lead sulfate are responsible for the observed phenomena.

Studies on the anodic dissolution of lead sulfide are very important as they give a fundamental understanding of the processes involved in developing methods for effective electrowinning of the metal from its sulfide. So far, much emphasis has been given on the perchlorate medium (1-8) for such dissolution studies. The industrial application of this highly oxidizing medium is not that attractive due to the accompanied formation of the insoluble oxides of lead. Attempts have been made in other media like fluoboric (9, 10), fluosilicic (10, 11), sulfuric (11, 12), hydrochloric (13, 14), and recently in sulfamic (15, 16) acids. Among these, fluoboric and fluosilicic acids have been eliminated by the investigators concerned (9-11) due to the fact that lead sulfide develops passivation in the earlier stages of the studies thus obstructing further observations. Similarly very little anodic dissolution is reported in a sulfuric acid (11) medium due to the very low solubility of the product, lead sulfate (k_{sp} 1.06×10^{-8} at 25°C) (17).

Sulfamic acid is attractive as a medium due to the high solubility (18) of the dissolution product, lead sulfamate, and the high dissolution rate (of lead sulfide) observed (15, 16). However, it creates problems due to slow hydrolysis (19) of the acid at room temperature (to ammonium bisulfate and then to ammonium sulfate) and also by the direct anodic oxidation of lead sulfide to lead sulfate (15, 16) especially at higher anodic potentials. This makes the sulfamic acid less productive industrially. Hydrochloric acid, on the other hand, is more viable due to the reason-

* Electrochemical Society Active Member.

Key words: electrowinning, electrodissolution, polarization, SEM.